

NEW APPARATUS & UPGRADES

OPTIMIZATION OF BEAMLINE BL41XU FOR MEASUREMENT OF MICRO-PROTEIN CRYSTAL

A number of protein crystallography techniques have been improved in recent years. With this advancement, many kinds of not only soluble protein but also biological important molecule such as protein complexes and membrane proteins have been analyzed. When such proteins are crystallized, it is difficult to obtain a crystal with a suitable size for the diffraction experiment ($\sim 100 \mu\text{m}$) though we commonly get a tiny crystal ($\sim 10 \mu\text{m}$). Therefore, in order to extend the range of an applicable crystal size ($< 20 \mu\text{m}$), it is necessary to establish the data collection method for such micro-sized crystals. There are various difficulties in acquiring diffraction data with high accuracy from such crystals. However, it is very important to make the size of the beam irradiated to the crystal equal to or smaller than the size of the crystal to reduce the component of a cryoprotectant solution in background scattering. At beamline **BL41XU**, the highly brilliant beam made by undulator enables us to perform a structural analysis of a 30- μm -size crystal. However, it is not optimized to such crystals because the beam size usually used is about $100 \times 100 \mu\text{m}^2$. Therefore, we have optimized the beamline setting from the second half of 2004, evaluating beam shape at the sample position.

We tuned up the optical components, such as a monochromator, focusing mirrors and two sets of quadrant slits, by evaluating the direct beam. As a result, the beam size of $25 \times 25 \mu\text{m}^2$ at the sample position was formed to at 1 \AA . However, the stability of beam intensity deteriorated markedly. The beam intensity in the beam size of $25 \times 25 \mu\text{m}^2$ decreased about 40% in 4 hours (Fig. 1) although the change in the intensity of the beam of $50 \times 50 \mu\text{m}^2$ is less than 2% within the same period. On the basis of results of the study, it is thought that this instability is caused by the thermal distortion of the double-crystal monochromator. Compton scattering generated by the first crystal heats and distorts the cradle of the second crystal. Therefore, we re-designed a "Compton shield" that was installed into the second cradle to remove such an effect, and introduced a new one (Fig. 2). Consequently, the change in beam intensity is suppressed to within 0.2% in 4 hours at the beam size of $25 \times 25 \mu\text{m}^2$ (Fig. 1). We also changed the aperture size of the front-end slit installed upstream of the monochromator. From the first half of 2005, the aperture size was reduced from $0.5 \times 0.5 \text{ mm}^2$ to $0.3 \times 0.3 \text{ mm}^2$ to improve the parallelity of the beam at a small beam size.

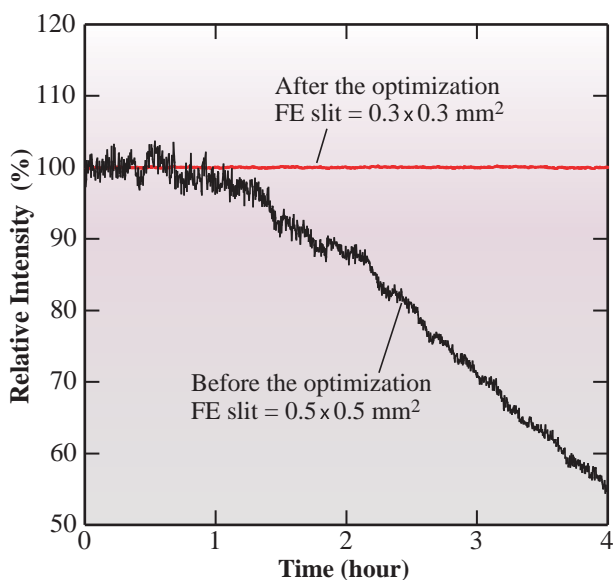


Fig. 1. Beam stability in beam size of $25 \times 25 \mu\text{m}^2$ at 1 \AA . These data were measured using pin-photodiode installed at sample position, and the measurement interval was 10 s.



Fig. 2. Compton shield (KOHZU Precision Co., Ltd.) installed to second cradle.

New Apparatus & Upgrades

As the result of these optimizations, the default beam size in BL41XU was changed from $100 \times 100 \mu\text{m}^2$ to $50 \times 50 \mu\text{m}^2$, and the $25 \times 25 \mu\text{m}^2$ beam became available for all users from the second half of 2005. Users can easily change the beam size only by selecting a target beam size from the GUI menu of the measurement software BSS [1]. The photon flux and photon density at the beam size of $25 \times 25 \mu\text{m}^2$ at 1 Å are 8.0×10^{10} photons/sec and 1.3×10^{14} photons/sec/mm², respectively. Figure 3 shows the

beam shape at the sample position. The beam size was adjusted using two sets of quadrant slits. The color of the solution changed only at the place where X-ray was irradiated. We are now executing test measurements using some typical crystals with a size of about 20 μm . The change in beam size would contribute to the improvement of the ratio of signal to background of diffraction images. We are going to optimize the beamline performance further on the basis of those results.

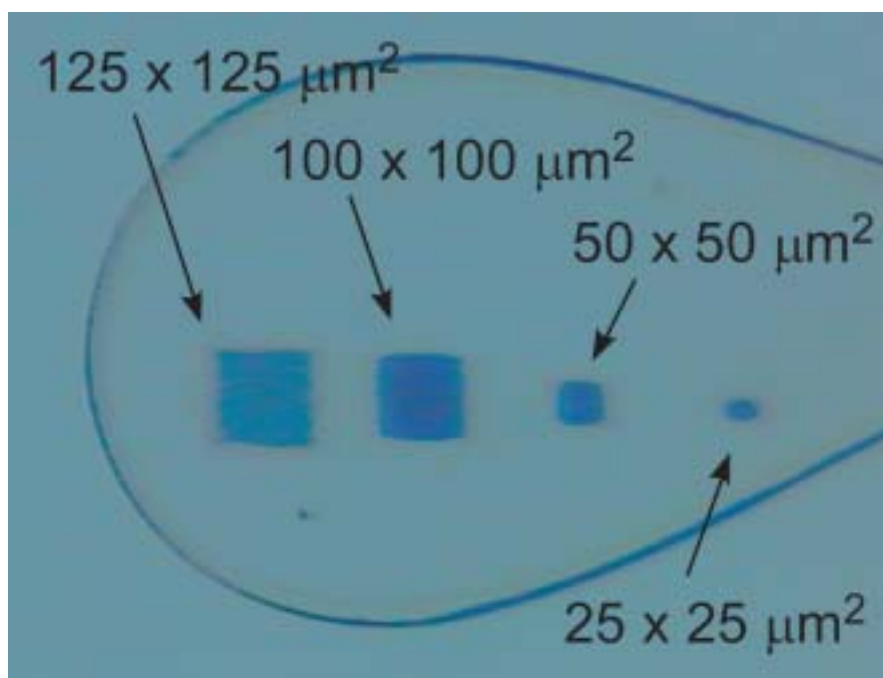


Fig. 3. Beam shape at sample position. This solution contains 30% glycerol and 30 % PEG4000.

Nobutaka Shimizu*, Kazuya Hasegawa and Masaki Yamamoto

SPring-8 / JASRI

*E-mail: nshimizu@spring8.or.jp

References

[1] G. Ueno, H. Kanda, T. Kumasaka and M. Yamamoto: J. Synchrotron Rad. **12** (2005) 380.

POWDER DIFFRACTOMETRY FOR TIME RESOLVED CHARGE DENSITY STUDY

Photo-induced phase transition is a phenomenon in which feeble light produces a marked change in the physical properties of materials. Photo-induced phases range from transient to persistent. It is well known that the persistent photo-induced phase transition is often accompanied by a crystal structural change [1]. Therefore, it has been believed that structure investigation is important for revealing the mechanism of photo-induced phase transition. However, in particular transient photo-induced structures have been hardly determined. One of the reasons of the difficulties is that only a tiny fraction of specimen can be induced by photo-irradiation. Therefore, a very small amount of specimen should be used to increase photo-excitation efficiency.

Thus, the high flux beamline **BL40XU** was selected for the time-resolved diffraction experiment. Synchrotron radiation has the aspects of not only high brilliance but also ultra-short pulse width. A time-resolved experiment only realizes when the pulse feature is utilized. The electrons in the storage ring go around at a frequency of 508 MHz. A magnetic levitation type mechanical chopper, called the X-ray Pulse Selector (XPS), was installed to select the voluntary electron bunch. The XPS is synchronized with the frequency of bunches. The maximum frequency of the XPS is 1 kHz. The time window of the XPS is approximately 500 ns. By combining the

chopper with the D-mode in SPing-8 as a bunch mode, a single bunch which has a pulse width of 40 ps can be extracted. The laser is triggered by the frequency of the XPS. The electric delay generator can control the delay time between the laser and X-ray. The schematic of this system is shown in Fig. 1.

BL40XU is not equipped with a monochromator, because this beamline adopts a quasi-monochromatic beam to maintain the photon flux. However, a monochromatic beam is indispensable for reduction of the powder profile's overlapping. Therefore a channel-cut monochromator is set up downstream of the chopper.

A monochromatic beam is irradiated onto the specimen on a powder diffractometer. The diffractometer for visualizing time-resolved charge densities was designed on the basis of the large Debye-Scherrer camera installed at beamline **BL02B2** [2]. The transient photo-induced phase has much instability. Whole powder patterns should be simultaneously measured. Accordingly, a two-dimensional detector, imaging plate, was attached to the camera. The mask with a 10-mm wide slit in front of the IP enables one to measure several data sets. By combining the multi-pattern recording system with the control program made by LabVIEW, the delay-time dependent data have been automatically obtained. Sample temperature is controlled from 90 K

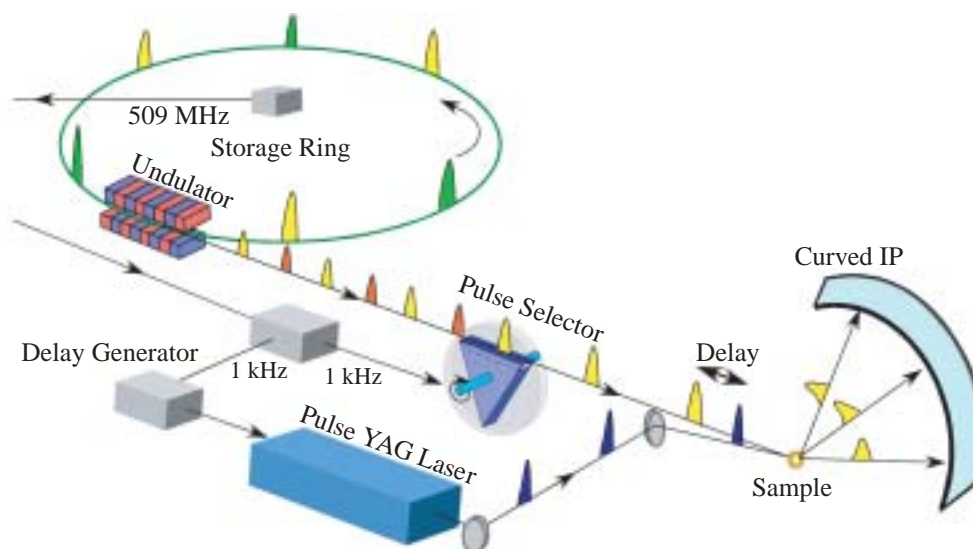


Fig. 1. Time-resolved experimental system using pump-probe method.

New Apparatus & Upgrades

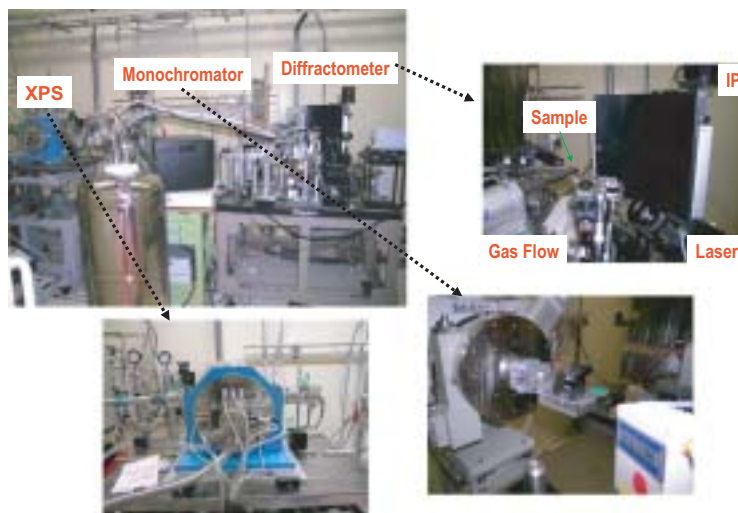


Fig. 2. X-ray pulse selector, channel cut monochromator and diffractometer installed at BL40XU.

up to 400 K using a nitrogen gas flow system.

Using the above time-resolved powder diffractometer shown in Fig. 2, we evaluated the reliability of the diffraction data obtained. As a result of Rietveld refinement for the standard sample CeO_2 , the time-resolved data is fit for accurate structural analysis. The reliability factor based on Bragg intensity was 1.6% and the profile is both symmetrical and sharp as

shown in Fig. 3.

We are now attempting to carry out time-resolved experiment with a 40 ps time resolution toward ultra-fast photo-sensitive materials at the charge density level.

The development of the experimental system has been performed during the long term proposal (Y. Moritomo *et al.*). The experimental know-how would be transferred to the CREST project (M. Takata *et al.*).

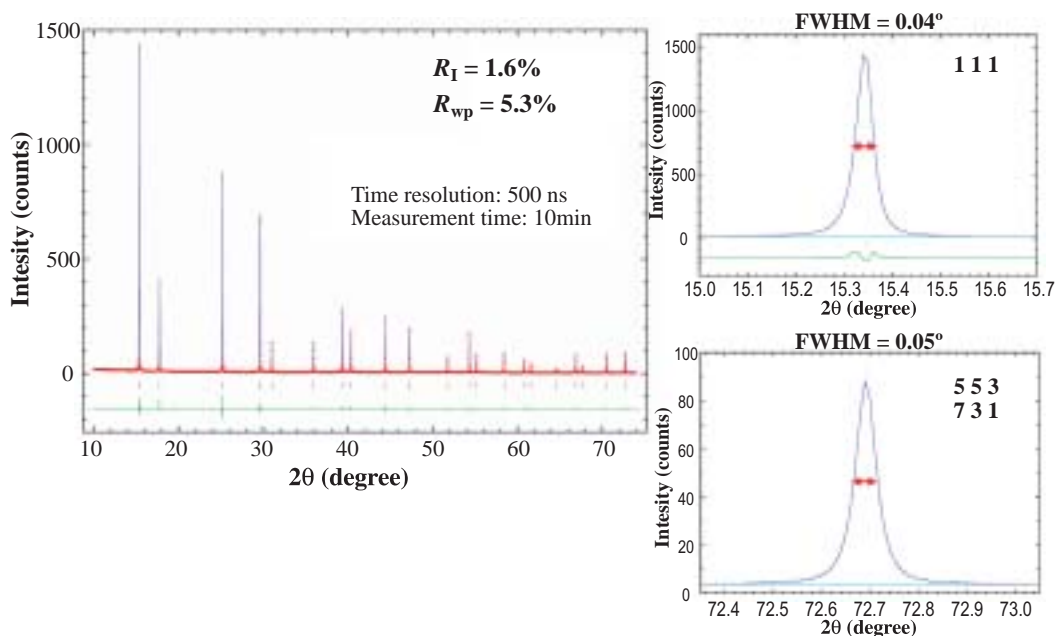


Fig. 3. The fitting results of Rietveld analysis for time-resolved data using standard sample, CeO_2 .

Kenichi Kato^{a,b}

^a SPring-8 / JASRI•RIKEN

^b CREST / JST

*E-mail: katok@spring8.or.jp

References

- [1] Y. Moritomo *et al.*: Phys. Rev. B **68** (2003) 144106.
- [2] Y. Moritomo and K. Kato: SPring-8 Information **11** (2006) 168; K. Kato and M. Takata: KEK Proc. 2005 **19** (2006) 114.

MICRO-AREA RECIPROCAL SPACE MAP MEASUREMENTS FOR CHARACTERIZING STRAIN STATUS OF EPITAXIAL LAYERS

Among X-ray diffraction techniques, the measurement of the distribution of intensity in a reciprocal space, the so-called reciprocal space map (RSM) measurement, is effective for characterizing the strain status of an epitaxial layer because lattice tilt is separated from lattice spacing [1]. If we can measure RSMs using an X-ray microbeam, it is expected to be a more powerful tool for characterizing local strain behavior in detail.

Microdiffraction systems using a zone plate (ZP) are suitable for characterizing the strain status of epitaxial layers [2,3]. This is because a hard X-ray microbeam produced by a ZP has both a sub-micrometer beam size and a relatively low angular divergence on the sub-milliradian order. However, this angular divergence is not sufficient for precise RSM measurements. We therefore developed a new high-angular-resolution X-ray microdiffraction system for RSM measurements.

The new diffractometer was installed at beamline **BL46XU** (Fig. 1). On this diffractometer, we employed a phase ZP as a focusing device. It contains 500-nm-thick gold zones with an innermost zone radius of 4 μm and an outermost zone width of 100 nm. The diameter of the ZP is 160 μm and number of zones is 400. For X-rays with an energy of 15 keV, the ZP is designed to have a large focal

length of 190 mm. The diffraction efficiency is about 3%. A 30- μm -diameter pinhole in a gold film was used as an order-sorting aperture (OSA). A 20- μm -wide slit was placed in front of the phase zone plate to partially irradiate the ZP. The center of the slit was off-placed 40 μm horizontally from the ZP center so that the OSA would eliminate unfocused and going-straight direct beam. This realized a focused beam with small size and small angular divergence. The beam size and angular divergence were measured to be 1.0 μm (horizontal) \times 2.8 μm (vertical), and 75 μrad , respectively. The sample stage consists of high precision stepping motor-driven stages including a $\theta - 2\theta$ rotation stage and XYZ linear stages, as well as two manual swivel stages on top. Those rotation stages have high angular resolutions of 1.7 and 8.7 μrad for the sample rotation (θ) and detector rotation (2θ), respectively. The linear stages have a minimum step size of 0.125 μm . To adjust the irradiation point on the sample precisely, the irradiation point was monitored using a long-focal-length optical microscope with a CCD camera. The maximum magnification of the microscope is 18 times. A detector was put on the 2θ arm. To improve the 2θ resolution, two sets of 20- μm -wide slits were placed in front of the detector.

Using this system, we tried to analyze the local

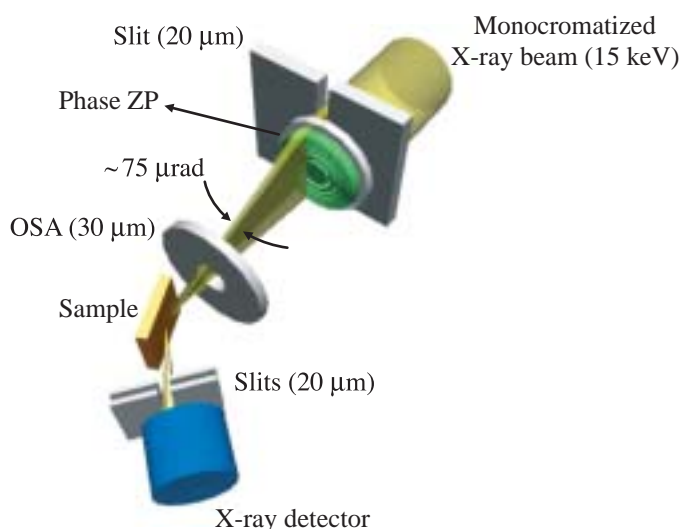


Fig. 1. Schematic figure of the experimental arrangement setup at BL46XU.

New Apparatus & Upgrades

strain and crystalline texture of strain-relaxed SiGe epitaxial films on Si(001) substrates, which have recently been attractive as buffer layers for high mobility strained Si channel electronic devices [4]. For example, Fig. 2 shows the measured RSM around the SiGe 004 diffraction spots of the sample, which had a total 125-nm-thick Si_{0.7}Ge_{0.3} layer on a Si(001) substrate. This is predominantly strain-relaxed with 60° misfit dislocations at the SiGe/Si(001) interface. It is found that every SiGe 004 diffraction peak

broadens along the Q_x direction. Furthermore, as shown by arrows in Fig. 2, several discrete peaks can be observed in the broadened SiGe 004 peak. These discrete peaks have never been observed without using the high-angular-resolution microdiffraction system. Detailed quantitative analysis revealed that crystal domains with sizes ranging from 100 nm to 140 nm at tilt angles from -0.18° to 0.42° with respect to the Si [001] direction are formed in the layer relaxed with 60° dislocations [4].

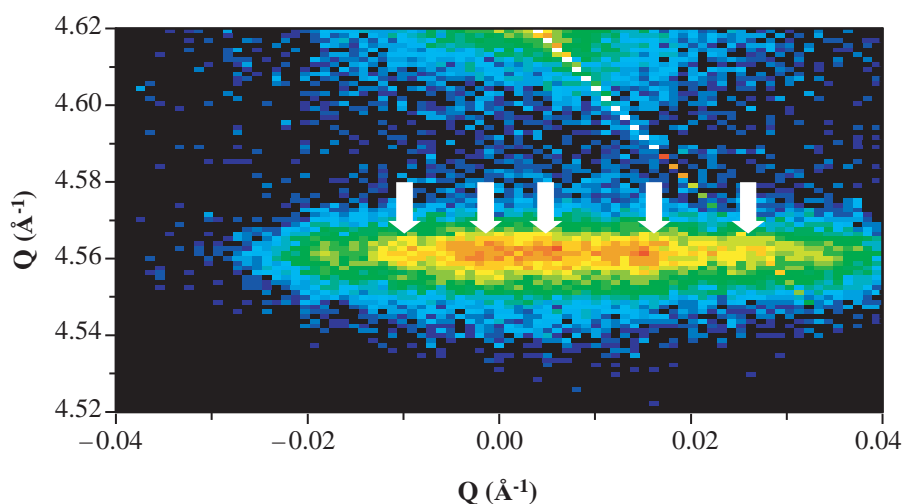


Fig. 2. Measured reciprocal space map around SiGe 004 diffraction spot.

Shigeru Kimura* and Shingo Takeda

JASRI / SPring-8

*E-mail: kimuras@spring8.or.jp

References

- [1] For a review, P. Fewster: *Semicond. Sci. Technol.* **8** (1993) 1915.
- [2] S. Kimura *et al.*: *Jpn. J. Appl. Phys.* **41** (2002) L1013.
- [3] S. Kimura *et al.*: *AIP Conference Proc.* **705** (2004) 1275.
- [4] S. Mochizuki, A. Sakai, N. Taoka, O. Nakatsuka, S. Takeda, S. Kimura, M. Ogawa and S. Zaima: *Thin Solid Films* **508** (2006) 128.

New Apparatus & Upgrades

DEVELOPMENT OF ULTRA-FAST CT SYSTEM WITH A QUASI-MONOCHROMATIC BEAM

An ultra-fast X-ray CT system was developed at beamline **BL40XU**. The beamline has a helical undulator as a light source and does not have any monochromator. Therefore, the bandwidth of the X-ray is 2 - 3 % and the total flux achieved is more than 10^{14} photons/sec, which is suitable for high-speed X-ray imaging. In particular, fast X-ray CT enables us to obtain four-dimensional information including time resolving ability. This is an important technology for all sciences.

The setup of the experiment is shown in Fig. 1. Two Pt-coated mirrors (200-mm-long) were placed in the experimental hutch. The mirrors were bent with a four-point bending mechanism. To make the X-ray field as even as possible, a beam diffuser was introduced upstream of the first mirror. This diffuser was made of a 5-mm-thick layer of graphite powder and rotated at speeds of 300 - 800 rpm. The image detector consisted of visible light conversion unit and a fast read-out CCD camera (Hamamatsu Photonics K.K.). The effective pixel size and format were $4.8 \mu\text{m} \times 4.8 \mu\text{m}$ and 656×494 pixels, respectively. The minimum measurement time was 10 s for 312 projections. The shortest interval between each measurement was about 3 min because it was necessary to store images on a hard disc.

A volume rendered image was successfully obtained using a fast CT system (Fig. 2). The sample was a toothpick. It took 15 s for the entire measurement. The X-ray energy was 15 keV. The number of projections was 411. The exposure time for each projection was 33 ms.

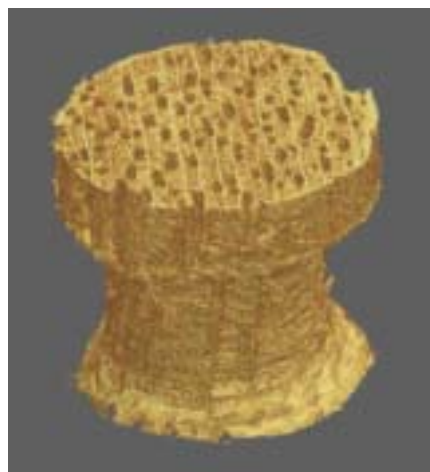


Fig. 2. Volume rendered image of part of a toothpick.

Kentaro Uesugi

SPring-8 / JASRI

E-mail: ueken@spring8.or.jp

References

- [1] K. Uesugi *et al.*: J. Synchrotron Rad. (2006) - to be published.

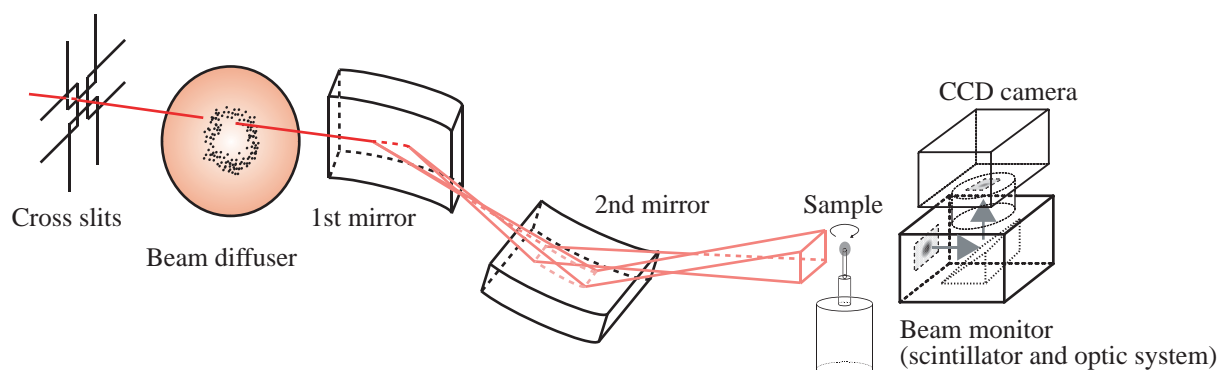


Fig. 1. Experimental setup.